Mechanical Properties of a Ferrofluid Seal: Three-Dimensional Analytical Study based on the Coulombian Model

Romain Ravaud, Guy Lemarquand

Machine Copy for Proofreading, Vol. x, y–z, 2008

MECHANICAL PROPERTIES OF A FERROFLUID SEAL: THREE-DIMENSIONAL ANALYTICAL STUDY BASED ON THE COULOMBIAN MODEL

R. Ravaud, G. Lemarquand

Laboratoire d'Acoustique de l'Universite du Maine, UMR CNRS 6613
Avenue Olivier Messiaen, 72085 Le Mans, France
guy.lemarquand@univ-lemans.fr

Abstract—This paper presents a general method for studying the mechanical properties of a ferrofluid seal by using a three-dimensional analytical approach based on the coulombian model of a magnet. The fundamental Maxwell's equations lead us to define the concept of magnetic energy of the ferrofluid seal by using only the three-dimensional equations of the magnetic field created by ring permanent magnets radially magnetized.

Our study corresponds to the specific case when the ferrofluid is submitted to a very high magnetic field. Under these conditions, the mechanical properties of the ferrofluid depend only on the magnetic field created by the permanent magnets. Throughout this paper, the remanence polarization J of the magnets used is higher than 1T. The magnetic field we use in order to align the magnetic particles is very intense, greater than 400 kAm^{-1}. Consequently, the magnetic particles are assumed to be saturated and the magnetic field they create can be omitted.

In this paper, a cylindrical structure consisting of two outer ring permanent magnets and an inner non-magnetic cylinder is considered. In addition, a ferrofluid seal is placed between them. The calculation of the magnetic pressure of the ferrofluid seal has been analytically established in three dimensions in order to determine its shape. Moreover, the geometrical evolution of the ferrofluid seal shape is presented when the inner non-magnetic cylinder crushes the ferrofluid seal. The radial stiffness of the ferrofluid seal is determined in three dimensions when the inner cylinder is decentered. Furthermore, a way of obtaining the ferrofluid seal static capacity is discussed.

It must be emphasized here that the three-dimensional method presented in this paper differs from the ones commonly used in the literature because the only term we consider in the equation of equilibrium describing the state of the ferrofluid seal is determined accurately. Such a method has been used for the design of ironless loudspeakers that have demonstrated some promising acoustical tests.

1. INTRODUCTION

Analytical calculations of the magnetic field produced by ring permanent magnets are useful for the design of devices using permanent magnets and ferrofluid seals. In this paper, we show how these analytical calculations can be used for studying and optimizing ferrofluid seals in ironless structures. To our knowledge, this way of studying a ferrofluid seal appears for the first time in the literature and we think that it can be useful for the design of magnetic bearings using ferrofluid seals or ironless loudspeakers.

Indeed, some recent papers dealing with ironless loudspeakers have clearly taken the same assumptions as the ones used in this paper for studying audio speakers containing ferrofluid [1]. The first studies dealing with ferrofluids were certainly carried out by Rosensweig [2] and many authors have been interested in the promising applications using ferrofluids [3].

On the other hand, some progress in the analytical calculations of the magnetic field produced by ring permanent magnets [4]-[12] have allowed us to determine accurately the magnetic energy of the ferrofluid by using the fundamental's Maxwell equations.

We can say that studies on ferrofluids deal generally with either their chemical and physical properties or their mechanical behavior [13]. Ferrofluids have various engineering applications [14], such as damping [15], for medical applications [16] or for ironless loudspeakers [17]-[19]. These last applications are the ones we are currently studying.

Moreover, ferrofluids are also often used as squeeze films [20] in bearings or as rotating shaft seals. Since then, numerous studies in the field of ferrofluid dynamic bearings have been carried out. Both static and dynamic characteristics of these bearings have been studied theoretically [21]-[29]. Moreover, recent trends in the ferrofluid lubrication applications are described and discussed, taking into account various

phenomena including cavitation -[34].

This paper presents a general method for studying the mechanical properties of a ferrofluid seal by using a three-dimensional analytical approach based on the coulombian model of a magnet. The structure considered is composed of two parts that are either made out of permanent magnets (the stator) or non magnetic materials (the moving part). Consequently, no reluctance effect is observed. The moving part has a translation movement, but this study does not take its effects into account. Thus, we only deal with the static properties of the ferrofluid seal. The magnetic field created by the ring permanent magnets is very intense. Therefore, the ferrofluid is largely saturated. Although numerical approaches are commonly used to study ferrofluid seals, analytical approaches with exact formulations allow a great flexibility in optimizing the dimensions of the configurations studied. Consequently, in our specific use of the ferrofluid seal, it is more interesting to use an exact analytical term rather than a lot of simplified terms in the Bernoulli equation for describing the state of the ferrolfuid seal.

It is noted that this study is entirely based on the magnetic pressure calculation which is analytical throughout this paper. Indeed, such an analytical approach allows a precise study of the ferrofluid seal shape when it is crushed, which is often an occurring state during the functioning. The seal capacity is also determined and discussed and a analytical method for obtaining the radial stiffness of the ferrofluid seal is also presented.

We think that this method paves the way for new and promosing applications using both permanent magnets and ferrofluid seals. All the analytical expressions used in this paper have been published in previous papers and are a good alternative to the finite element method for the design of such structures.

2. STRUCTURE DESCRIPTION

2.1. Geometry

The studied structure consists of two outer ring permanent magnets and an inner non-magnetic cylinder. Such a structure is considered in this paper because it allows us to have important gradient values. Moreover, this structure is not very complicated to build since it requires only two ring permanent magnets. As a result, the magnets are stacked and their magnetizations are both radial, but in opposed directions (Fig.1). The non-magnetic cylinder is centered with the two ring permanent magnets. Moreover, both outer ring permanent

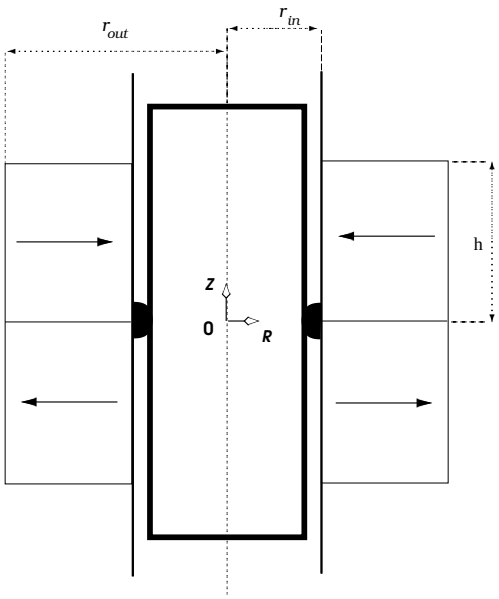

Figure 1. Geometry : two outer ring permanent magnets and an inner non-magnetic cylinder with a ferrofluid seal between them; the ring inner radius is r_{in}, the ring outer radius is r_{out}, the height of a ring permanent magnet is h.

magnets have the same dimensions and the same magnetization in magnitude. The ring inner radius is r_{in}, the ring outer radius is r_{out} and the ring permanent magnet height is h. The z axis is a symmetry axis.

2.2. Basic equations

The magnetic field produced by the ring permanent magnets can be determined by using a fully analytical approach. The fundamental equations of Maxwell lead us to determine the magnetic energy in the ferrofluid. Indeed, let us consider the four fundamental Maxwell's equations:

$$\vec{\nabla}.\vec{B} = 0 \tag{1}$$

$$\vec{\nabla} \wedge \vec{H} = \vec{j} \tag{2}$$

$$\vec{\nabla}.\vec{D} = \rho \tag{3}$$

$$\vec{\nabla} \wedge \vec{E} = -\frac{\partial \vec{B}}{\partial t} \tag{4}$$

where $\vec{B}$ is the magnetic induction field, $\vec{H}$ is the magnetic field, $\vec{j}$ is the volume current density, $\vec{D}$ is the electric flux density, $\vec{E}$ is the electrostatic field and ρ is the electrical charge. In our structure, no currents are considered as the magnetic field is created only by the permanent magnets. The vector fields $\vec{B}$ and $\vec{H}$ are defined for all points in space with the following relation:

$$\vec{B} = \mu_0 \vec{H} + \vec{J} \tag{5}$$

where μ_0 is the permeability of the vacuum and $\vec{J}$ is the polarization vector of the magnet. When the magnetic field is determined outside of the magnet, we have $\vec{J} = \vec{0}$. The analogy between the Mawxell's equations leads us to write that:

$$\vec{\nabla}.\vec{H} = -\frac{\vec{\nabla}.\vec{J}}{\mu_0} = \frac{\sigma^*}{\mu_0} \tag{6}$$

where σ^* corresponds to a fictitious magnetic pole density. On the other hand, the magnetic field $\vec{H}$ verifies the following equation:

$$\vec{\nabla} \wedge \vec{H} = \vec{0} \tag{7}$$

Thus, $\vec{H}$ can de deducted from a scalar potential $\phi(\vec{r})$ by

$$\vec{H} = -\vec{\nabla}\left(\phi(\vec{r})\right) \tag{8}$$

Let us consider a structure owing several ring permanent magnets, that is, an assembly of magnetic pole surface densities and magnetic pole volume densities; with (6) and (7), we can write that

$$\phi(\vec{r}) = \frac{1}{4\pi\mu_0}\left(\sum_i \int\int_{S_i} \frac{\vec{J_k}.d\vec{S_i}}{\left|\vec{r}-\vec{r'}\right|} + \sum_j \int\int\int_{V_j} \frac{-\vec{\nabla}.\vec{J_k}}{\left|\vec{r}-\vec{r'}\right|} dV_j\right) \tag{9}$$

where $\vec{J_k}$ is the magnetic polarization vector owing to the ring permanent magnet k and $\left|\vec{r}-\vec{r'}\right|$ is the distance between the observation point and a magnetic charge contribution. We deduct immedialtely that the magnetic field created by the ring permanent magnets is determined as follows:

$$\vec{H} = -\vec{\nabla}.\left(\frac{1}{4\pi\mu_0}\left(\sum_i \int\int_{S_i} \frac{\vec{J_k}.d\vec{S_i}}{\left|\vec{r}-\vec{r'}\right|} + \sum_j \int\int\int_{V_j} \frac{-\vec{\nabla}.\vec{J_k}}{\left|\vec{r}-\vec{r'}\right|} dV_j\right)\right) \tag{10}$$

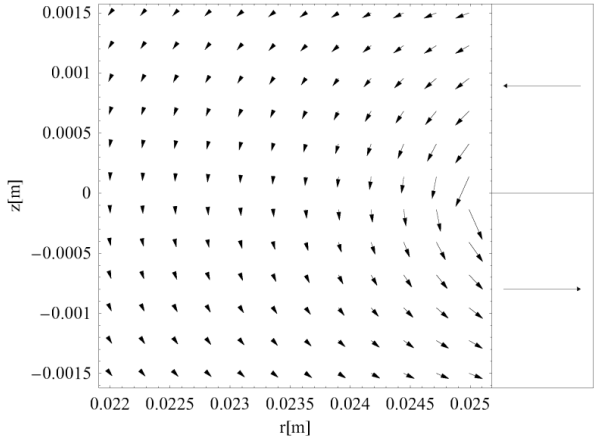

Figure 2. Magnetic field created by the two outer ring permanent magnets; $r_{in} = 25$ mm, $h = 3$ mm, $\sigma^* = 1$ T

As there is a cylindrical symmetry in our configuration, the magnetic field depends only on two variables r and z. This relation is used in the next section for showing the magnetic field in our configuration.

2.3. Magnetic field created by the two ring permanent magnets

As shown in Fig 1, our geometry is comoosed of two ring permanent magnets. The magnetic field created by the two outer ring permanent magnets depends on both the radius, r, and the altitude, z. The radial component of the magnetic field created by the two outer ring permanent magnets is denoted $H_r(r, z)$ and the axial component is denoted $H_z(r, z)$. It is noted that the expressions of these components have been established in previous papers [9]-[11]. The magnetic field $\vec{H}$ is represented in Fig.2. The ring inner radius r_{in} equals 25 mm, the ring outer radius equals 28 mm and the permanent magnet height, h, equals 3 mm. The magnetic pole surface density $+\sigma^*$ equals 1 T. Figure 2 shows that the magnetic field $\vec{H}$ is the strongest near the permanent magnets, especially where the magnetic field gradient is the most important.

3. MAGNETIC PRESSURE ON THE FERROFLUID SEAL

3.1. Assumptions

It is emphasized that the structure considered in this paper contain no iron. Moreover, the further calculations are presented for magnets with 1 T remanent magnetization in order to normalize the results. In fact, the magnets used in the prototypes are Neodymium Iron Boron ones for which the remanent magnetization can reach 1.5 T. Furthermore, the interesting regions of space are the ones where the ferrofluid goes. Besides, in the field gradient due to the external magnetic field created by the two outer ring permanent magnets, the magnetic particles are attracted towards the higher intensity regions of the magnetic field. With these 1 T normalized magnets and for the proposed configurations, the magnetic field intensity there is greater than 400 kA/m. Of course, all the field values are proportional to remanent magnetization value.

Then, we use commercial ferrofluids either from the company Ferrotec or Ferrolabs. Such ferrofluids have a saturation magnetization, M_s, smaller than 32 kA/m and a particle concentration below 5.5 %. It is to be noted that for bearing or loudspeaker applications, a great bearing effect is seeked which requires high saturation magnetizations. Therefore, the magnetic field, $\vec{H}$, created by the permanent magnets is far higher than the ferrofluid critical field [35]. So, the ferrofluid is totally saturated and its magnetization is denoted M_s. Another consequence is that the magnetic relative permeability of the ferrofluid equals one. Thereby, the presence of ferrofluid does not modify the magnetic field created by the permanent magnets and the field created by the ferrofluid itself is omitted. Moreover, the ferromagnetic particles are assumed to be small saturated spheres which can be freely oriented in all the directions of space. Besides, this study is a static one. Thus, all the particles of the saturated ferrofluid are aligned with the permanent magnet orienting field. Consequently, the ferrofluid magnetization has the same direction as the orienting field. Furthermore, the aggregation in chains of the ferrofluid particles is omitted [36]. It is noted that, when the device is at laboratory temperature and at rest, the aggregation phenomenon is observed.

Moreover, the thermal energy E_T ($E_T = kT$ where k is Boltzmann's constant and T is the absolute temperature in degrees Kelvin) and the gravitational energy E_G ($E_G = \Delta\rho V g L$ where V is the volume for a spherical particle, L is the elevation in the gravitational field, g is the standard gravity, $\Delta\rho$ is the difference between the ferrofluid density and the outer fluid) are neglected.

Eventually, this paper deals with the ferrofluid free boundary surface. Its shape depends on the result of the force competition at this boundary. On one hand, the magnetic pressure, p_m, is exerted. It is given by:

$$p_m(r,z) = \mu_0 \mathbf{M_s}.\vec{H}(r,z) = \mu_0 M_s \sqrt{H_r(r,z)^2 + H_z(r,z)^2} \qquad (11)$$

where both magnetic field components $H_r(r,z)$ and $H_z(r,z)$ are analytically calculated [9]. It is to be noted that this expression is given below in a fundamental form. However, this expression can be written in a form more suitable for numerical treatments [4]. The magnetic pressure $p_m(r,z)$ is given by (12).

$$p_m(r,z) = \mu_0 M_s \sqrt{H_r(r,z)^2 + H_z(r,z)^2} \qquad (12)$$

where M_s is the intensity of magnetization of a magnetic particle. The radial component $H_r(r,z)$ of the magnetic field created by the two permanent magnets is defined by (13).

$$H_r(r,z) = \frac{\sigma^*}{\pi\mu_0} i(1+u)\left(\varsigma(u_1) - \varsigma(u_2)\right) \qquad (13)$$

with

$$\begin{aligned}
\varsigma(u) \;=\; & \frac{\xi_1(-(a_1 d + b_1(c+e_1)))F^*\left[i\sinh^{-1}[\frac{\sqrt{-c+d-e_1}}{\sqrt{c+e_1+du}}], \frac{c+d+e_1}{c-d+e_1}\right]}{d\sqrt{-c+d-e_1}e_1\sqrt{\frac{d(1+u)}{c+e_1+du}}\sqrt{1-u^2}} \\
& + \frac{\xi_1(b_1 c - a_1 d)\Pi^*\left[\frac{e_1}{c-d+e_1}, i\sinh^{-1}[\frac{\sqrt{-c+d+e_1}}{c+e_1+du}], \frac{c+d+e_1}{c-d+e_1}\right]}{d\sqrt{-c+d-e_1}e_1\sqrt{\frac{d(1+u)}{c+e_1+du}}\sqrt{1-u^2}} \\
& + \frac{\xi_2\left(-(a_2 d + b_2(c+e_2))\right)F^*\left[i\sinh^{-1}[\frac{\sqrt{-c+d-e_2}}{\sqrt{c+e_2+du}}], \frac{c+d+e_2}{c-d+e_2}\right]}{d\sqrt{-c+d-e_2}e_2\sqrt{\frac{d(1+u)}{c+e_2+du}}\sqrt{1-u^2}} \\
& + \frac{\xi_2(b_2 c - a_2 d)\Pi^*\left[\frac{e_2}{c-d+e_2}, i\sinh^{-1}[\frac{\sqrt{-c+d+e_2}}{c+e_2+du}], \frac{c+d+e_2}{c-d+e_2}\right]}{d\sqrt{-c+d-e_2}e_2\sqrt{\frac{d(1+u)}{c+e_2+du}}\sqrt{1-u^2}} \\
& - \frac{\eta_3\left((a_3 d - b_3 e_3)\right)F^*\left[i\sinh^{-1}[\frac{\sqrt{-d-e_3}}{\sqrt{e_3+du}}], \frac{-d-e_3}{d+e_3}\right]}{d\sqrt{-d-e_3}(-c+e_3)\sqrt{\frac{d(1+u)}{e_3+du}}\sqrt{1-u^2}} \\
& - \frac{\eta_3(b_3 c - a_3 d)\Pi^*\left[\frac{-c+e_3}{d+e_3}, i\sinh^{-1}[\frac{\sqrt{-d+e_3}}{e_3+du}], \frac{-d+e_3}{d+e_3}\right]}{d\sqrt{-d-e_3}(-c+e_3)\sqrt{\frac{d(1+u)}{e_3+du}}\sqrt{1-u^2}}
\end{aligned}$$

$$-\frac{\eta_4\left(a_4d-b_4e_4\right)F^*\left[i\sinh^{-1}[\frac{\sqrt{-d-e_4}}{\sqrt{e_4+du}}],\frac{-d+e_4}{d+e_4}\right]}{d\sqrt{-d-e_4}(c+e_4)\sqrt{\frac{d(1+u)}{e_4+du}}\sqrt{1-u^2}}$$
$$-\frac{\eta_4(b_4c-a_4d)\Pi^*\left[\frac{-c+e_4}{d+e_4},i\sinh^{-1}[\frac{\sqrt{-d-e_4}}{e_4+du}],\frac{-d+e_4}{d+e_4}\right]}{d\sqrt{-d-e_4}(-c+e_4)\sqrt{\frac{d(1+u)}{e_4+du}}\sqrt{1-u^2}} \tag{14}$$

The axial component of the magnetic field created by the two ring permanent magnets is given by (15).

$$\begin{aligned} H_z(r,z) &= \frac{\sigma^*}{\pi\mu_0}\left(-r_{in}\frac{K^*\left[\frac{-4rr_{in}}{(r-r_{in})^2+z^2}\right]}{\sqrt{(r-r_{in})^2+z^2}}\right) \\ &+\frac{\sigma^*}{\pi\mu_0}\left(r_{in}\frac{K^*\left[\frac{-4rr_{in}}{(r-r_{in})^2+(z-h)^2}\right]}{\sqrt{(r-r_{in})^2+(z-h)^2}}\right) \\ &-\frac{\sigma^*}{\pi\mu_0}\left(r_{in}\frac{K^*\left[\frac{-4rr_{in}}{(r-r_{in})^2+z^2}\right]}{\sqrt{(r-r_{in})^2+z^2}}\right) \\ &+\frac{\sigma^*}{\pi\mu_0}\left(r_{in}\frac{K^*\left[\frac{-4rr_{in}}{(r-r_{in})^2+(z+h)^2}\right]}{\sqrt{(r-r_{in})^2+(z+h)^2}}\right) \end{aligned} \tag{15}$$

$$\xi_i=\sqrt{\frac{d(-1+u)}{c+e_i+du}} \tag{16}$$

$$\eta_i=\sqrt{\frac{d(-1+u)}{e_i+du}} \tag{17}$$

where $K^*[m]$ is given in terms of the incomplete elliptic integral of the first kind by (18)

$$K^*[m]=F^*[\frac{\pi}{2},m] \tag{18}$$

$F^*[\phi,m]$ is given in terms of the elliptic integral of the first kind by (19):

$$F^*[\phi,m]=\int_{\theta=0}^{\theta=\phi}\frac{1}{\sqrt{1-m\sin(\theta)^2}}d\theta \tag{19}$$

Parameters	
a_1	$r_{in}rz$
b_1	$\text{-}r_{in}^2 z$
c	$r^2 + r_{in}^2$
d	$-2rr_{in}$
e_1	z^2
a_2	$-r_{in}r(z-h)$
b_2	$r_{in}^2(z-h)$
e_2	$(z-h)^2$
a_3	$r_{in}rz$
b_3	$-r_{in}^2 z$
e_3	$r^2 + r_{in}^2 + z^2$
a_4	$r_{in}r(-z-h)$
b_4	$-r_{in}^2(-z-h)$
e_4	$r^2 + r_{in}^2 + (z+h)^2$

Table 1. Definition of the parameters used in (14)

$\Pi^*[n, \phi, m]$ is given in terms of the incomplete elliptic integral of the third kind by (20)

$$\Pi^*[n, \phi, m] = \int_0^{\phi} \frac{1}{(1 - n\sin(\theta)^2)\sqrt{1 - m\sin(\theta)^2}} d\theta \qquad (20)$$

The parameters used in (14) are defined in Table 1. Moreover, when we input (13) in Mathematica, we have to take the real part of $H_r(r, z)$ because of the noise calculus. What's more, the parameter i used in (14) is the imaginary number ($i^2 = -1$).

As the ferrofluid considered in this paper has a saturation magnetization of 32 kA/m and the magnetic field is greater than 400 kA/m, the value of this pressure is higher than 12800 N/m^2. On the other hand, the surface tension exists. But when the values of both the surface tension coefficient, A, (A equals 0.0256 kg/s^2 for the used ferrofluids) and the radius of curvature are considered, the effect of the surface tension can be omitted: this latter does not deform the free boundary surface.

Finally, for hydrodynamic pressures which equal zero or have low values, the seal free boundary surface is a magnetic iso-pressure surface. Then, its mechanical properties, such as its capacity or its stiffness can be studied. Further dynamic studies could also be carried out with a perturbation method from this rest position [37].

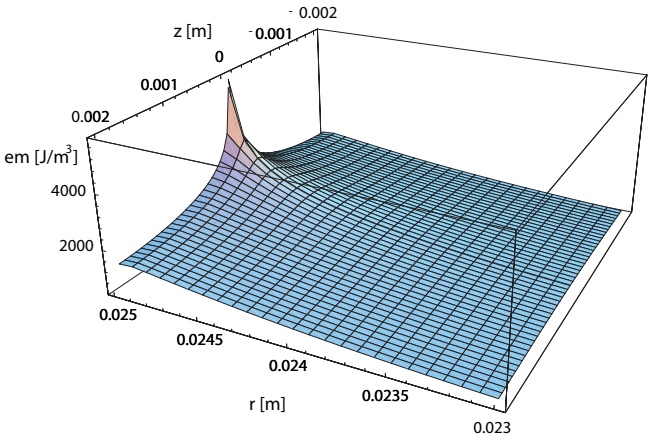

Figure 3. Three-dimensional representation of the magnetic pressure of the ferrofluid seal

3.2. Three-dimensional representation of the magnetic pressure

Figure 3 represents the magnetic pressure layer of the ferrofluid seal. The magnetic pressure $p_m(r, z)$ has been determined with (11). Figure 3 shows that the magnetic pressure is greater near the two ring permanent magnets, especially where the magnetic field gradient is the strongest. It can be noted that such a figure is useful to see quickly where the magnetic pressure is the most important. Moreover, Fig. (3) gives also an indication about how the magnetic pressure varies according to r and z; we see that this variation is very important either to the permanent magnets. Furthermore, this representation is interesting since it shows that the potential energy is concentrated in a very small ferrofluid volume. As a consequence, it gives an indication about what quantity of ferrofluid should be used to design a ferrofluid seal. Indeed, some viscous effects can appear when the inner cylinder moves between the two outer ring permanent magnets. If a large quantity of ferrofluid is used, the ferrofluid seal is thick, the potential energy increases but the viscous effects become an actual drawback according to the dynamic movement of the inner cylinder. If a too small amount of ferrofluid is used, the viscous effects disappear but all the interesting properties of the ferrofluid seal (damping, stability, linearity,...) disappear as well. In short, to a given geometry (here two ring permanent magnets with an inner non-magnetic cylinder) corresponds to an adequate quantity of ferrofluid which has some

interesting physical properties with very little viscous effects.

3.3. Potential energy of the ferrofluid seal

The potential energy of the ferrofluid seal is defined by (21):

$$E_m = -\int\int\int_{(\Omega)} p_m(r,z)dV \tag{21}$$

where (Ω) is the ferrofluid seal volume. Indeed, this energy allows the calculation of the seal mechanical properties. As a remark, the magnetic pressure is given in N/m^2 and the potential energy in J.

4. STUDY OF THE FERROFLUID SEAL SHAPE

4.1. Ferrofluid seal shape under a magnetic field

We first analyze the ferrofluid shape without taking into account the inner non-magnetic cylinder. As we assume each magnetic particle to be a small sphere which can be freely oriented in all the directions of space, each magnetic particle is oriented with the direction of the orienting field in order to minimize its potential magnetic energy. More exactly, the magnetic particles go where the magnetic field is the most important by always being aligned with it. Figure 4 is a two dimensional contour representation of the potential energy of the ferrofluid seal. Such a figure is useful to see the points in space which have the same potential energy. This is interesting because this element of information allows us to study the deformation of the seal when the inner cylinder is radially decentered.

The aim of this figure is to show where the ferrofluid goes at first: the warmest areas are the first occupied ones. The shape of the ferrofluid seal between $r = 24.6$ mm and $r = 25$ mm can be approximated as half an ellipse. Consequently, when the ferrofluid seal thickness is smaller than 0.4 mm, its contour can be written in terms of an equation of an ellipse (22).

$$\frac{(r-r_i)^2}{a_i^2} + \frac{z^2}{b_i^2} = 1 \tag{22}$$

To illustrate (22), Table (2) gives the parameters of the equations of ellipse describing the ferrofluid seal in Fig.4 for r between 24.6 mm and 25 mm. The approximation error between the equations of ellipse and the real contour shape of the ferrofluid seal is also given. When some ferrofluid is added, the shape of the ferrofluid seal changes and for

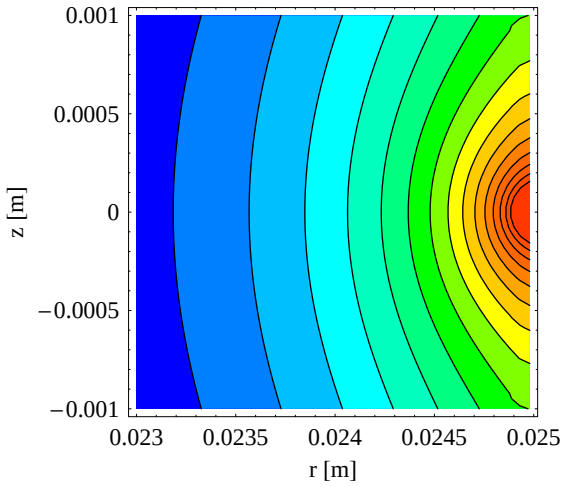

Figure 4. Representation of growing ferrofluid volumes under a magnetic field from the warmest areas to the coolest ones; the warmest colors correspond to the region in space where the magnetic energy is the strongest

Ellipse	$\mathbf{a_i}$	$\mathbf{b_i}$	$\mathbf{r_i}$	**error**
$5\%E$	0.25	0.275	25	0.5%
$10\%E$	0.27	0.297	25	0.9%
$15\%E$	0.29	0.319	25	1.4%

Table 2. Parameters (in mm) of the equations of an ellipse describing small ferrofluid seals

$r < 24.6$ mm, as represented in Fig.5, the ferrofluid seal contour cannot be represented in terms of an equation of ellipse. Furthermore, we can point out that if a large amount of ferrofluid is added, the ferrofluid seal size becomes very large because of the magnet edge effects. In our configuration, the thickness of the ferrofluid seal for which the shape changes is 0.6 mm. This element of information is very important since it gives clearly what quantity of ferrofluid sould be used to make a small seal. We have also represented the final three-dimmensional form of the ferrofluid seal with the same dimensions (r_{in}= 25 mm. $J = 1$ T, $h = 3$ mm) in Fig 6.

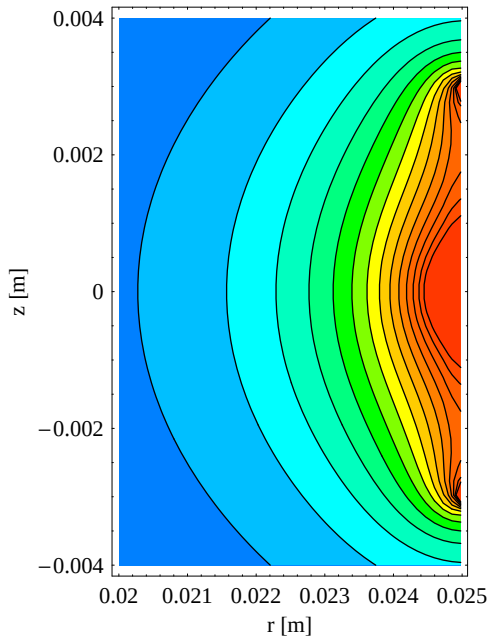

Figure 5. Representation of growing ferrofluid volumes under a magnetic field from the warmest areas to the coolest ones: the warmest colors correspond to the region in space where the magnetic energy is the strongest

4.2. Shape of the crushed ferrofluid seal

We take now the non-magnetic cylinder into account. The device has to be dimensioned in such a way so that the cylinder crushes the seal, in order to reach the intended watertightness. Figure 7 shows where the ferrofluid goes when the inner non-magnetic cylinder crushes the ferrofluid seal. The phenomenon is axisymmetrical, as the inner cylinder is supposed here to be centered. As seen in Fig. 4, for small quantities of ferrofluid, the ferrofluid seal contour can be described in terms of an equation of ellipse. Therefore, when a small ferrofluid seal is crushed, the quantity of ferrofluid goes symmetrically under and above the initial ferrofluid seal by describing an equation of ellipse.

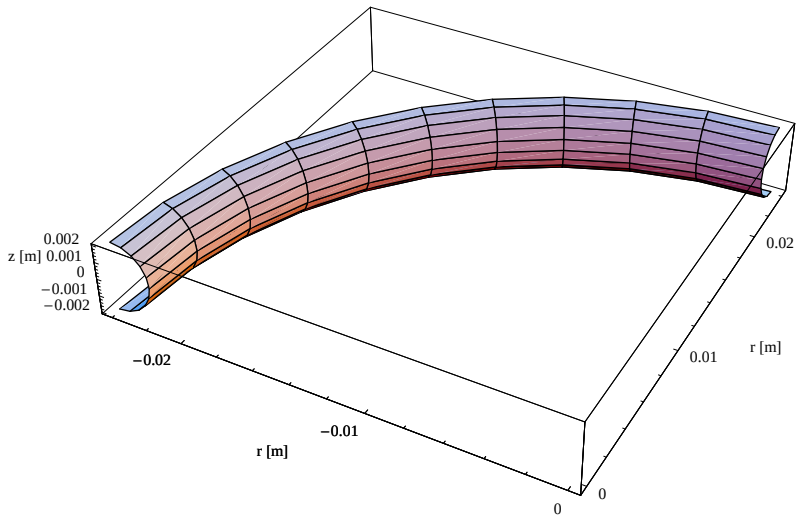

Figure 6. Tree-dimensional representation of the ferrofluid seal volume; the ring inner radius equals 25 mm. $J = 1$ T, $h = 3$ mm

Displacement	Energy reduction
$0,1$ mm	13%
$0,15$ mm	35%
$0,2$ mm	68%

Table 3. The energy reduction is a function of the radial displacement of the inner cylinder

This ellipse is truncated because of the inner non-magnetic cylinder. The change of the ferrofluid seal shape generates an energy reduction. Table 3 presents the energy reduction when the cylinder, being first at a distance in length which equals 0.3 mm from r_{in}, crushes radially the ferrofluid seal. The energy reduction is very important (68%) when the radial displacement of the inner cylinder is 0.2 mm.

5. CALCULATION OF THE STATIC CAPACITY OF THE FERROFLUID SEAL

The aim of this section is to determine the ferrofluid seal static capacity. Indeed, the pressure underneath the non-magnetic cylinder can be

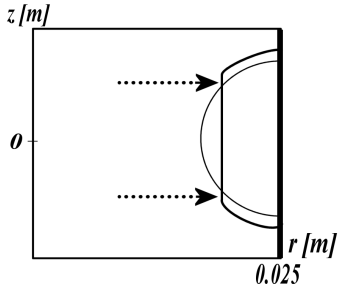

Figure 7. Ferrofluid seal which is crushed

very different from the pressure above the non-magnetic cylinder. Consequently, a pressure gradient appears and the ferrofluid seal is thus deformed. Therefore, the calculation of the ferrofluid seal capacity is required. For this purpose, a second configuration is considered, which corresponds to the case when a cylindrical air gap appears in the seal along the cylinder because of an applied pressure on one side of the seal. This second configuration is represented in Fig.8. Two steps are necessary to determine the capacity of the ferrofluid seal. The first step is the determination of the potential energy of the ferrofluid seal without any air gap in the seal. To do so, a numerical integration of (21) leads to a first value of the potential energy which is denoted $E_m(1)$. The used numerical method is the GaussKronrod method. A three-dimensional representation of the ferrofluid seal perfored in shown in Fig 9. The second step is the determination of the potential energy of the ferrofluid seal with the air gap. Again, a numerical integration leads to a second value of the potential energy denoted $E_m(2)$. The energy difference is denoted ΔE_m and verifies (23):

$$\Delta E_m = E_m(1) - E_m(2) \tag{23}$$

The energy difference corresponds to the pressure work $\delta W(P)$ and satisfies (24):

$$\Delta E_m = \delta W(P) = PSd \tag{24}$$

where S is the surface area of the air gap and d is the thickness of the perforation. Consequently, the capacity P_{lim} verifies (25):

$$P_{lim} = \frac{\delta W(P)}{Sd} \tag{25}$$

A numerical application has been done with several ring inner radii (Fig.10). We define the ferrofluid thickness as the thickness of the

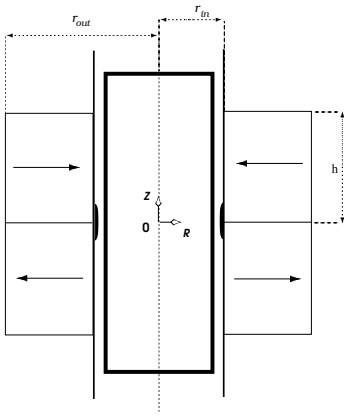

Figure 8. Geometry: two ring permanent magnets and an inner non-magnetic cylinder; air gap in the seal

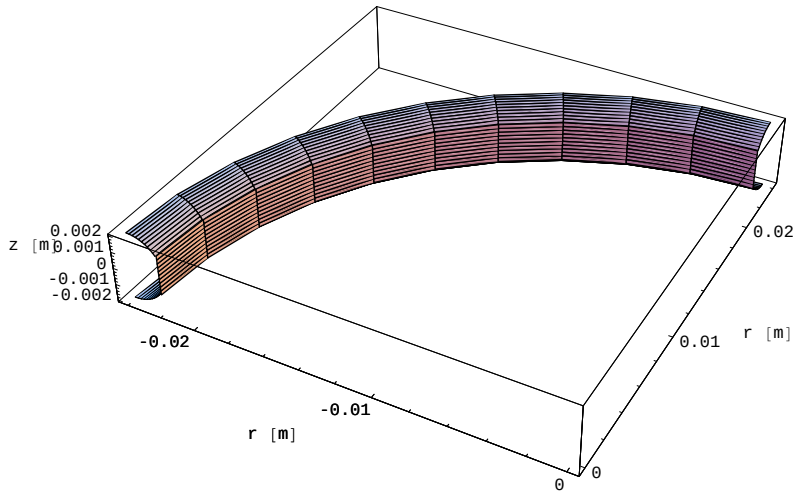

Figure 9. Tree-dimensional representation of the ferrofluid seal that is crushed; the ring inner radius equals 25 mm. $J = 1$ T, $h = 3$ mm

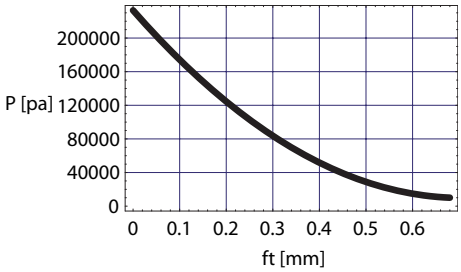

Figure 10. The static limit pressure P [Pa] is a function of the ferrofluid seal thickness ft [mm]

Ferrofluid thickness	Volume	Hlim
$0,1$ mm	$4.7.10^{-9}$ m^3	700 000 A/m
$0,3$ mm	$2.1.10^{-8}$ m^3	600 000 A/m
$0,5$ mm	$1.2.10^{-8}$ m^3	450 000 A/m

Table 4. Volume and Magnetic field corresponding to a given ferrofluid thickness

ferrofluid between the outer ring permanent magnets and the inner cylinder. Figure 10 shows that the thinner the ferrofluid seal is, the higher the pressure gradient to which the ferrofluid seal can resist is. Table 4 gives both the volume corresponding to each ferrofluid thickness and the smallest magnetic field $Hlim$ in the concerned volume.

6. RADIAL STIFFNESS OF THE FERROFLUID SEAL

6.1. Determination of the radial stiffness

This section presents a way of obtaining the radial stiffness of the ferrofluid seal. For this purpose, a third configuration is considered (Fig.11), which corresponds to a decentered inner cylinder. Figure 12 illustrates the dependence of the radius with θ. The ferrofluid seal is thus more crushed when the cylinder comes closer to the magnets. The problem here is no longer axisymmetrical, but fully three-dimensional. Indeed, where the radial room for the ferrofluid is narrower, the seal becomes larger along the Oz axis, but the ferrofluid also moves towards the region of increasing room and so, the angle θ interferes. The way of obtaining the radial stiffness is done in two steps.

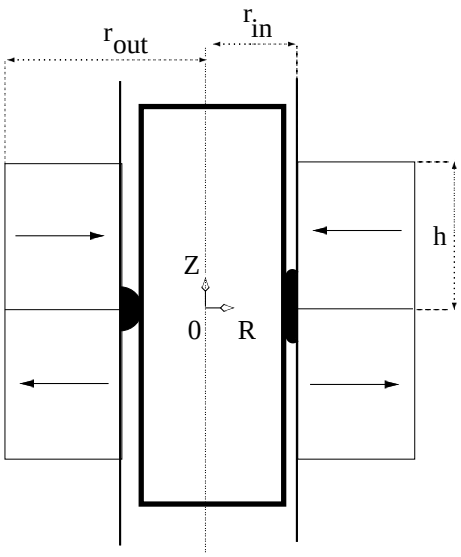

Figure 11. Radially moved away cylinder, crushed ferrofluid

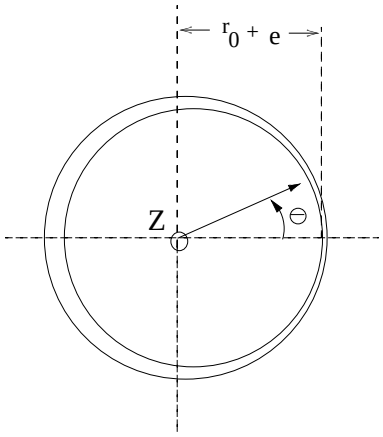

Figure 12. Cross-section of the radially moved away cylinder

The potential energy $E_m(1)$ is first calculated when the non-magnetic cylinder is centered (Fig.1) with (21). Then, the potential energy $E_m(2)$ is calculated when the non-magnetic cylinder is not centered (Fig.11). In the second configuration, the limits of the integrals which allow us to determine the potential energy depend on the angle θ. Consequently, the potential energy $E_m(2)$ is determined with (26).

$$E_m(2) = \int_0^{2\pi} \int_{r_0+e\cos(\theta)}^{r_{in}} \int_{-z_0}^{z_0} e_m(r,z) r dr d\theta dz \tag{26}$$

where r_0 and e are determined by the equation of the circle which is not centered given by (27).

$$r(\theta) = r_0 + e\cos(\theta) \tag{27}$$

where $r_0 = 24.7$ mm and $e = 0.1$ mm. Figure 12 shows how the inner cylinder is decentered. Consequently, the ferrofluid shape is not axisymmetrical since the inner cylinder is radially decentered.

As the ferrofluid shape is not axisymmetrical, the limits of the integrals in Eq. 26 depend on the angle θ. Thanks to the determination of $E_m(1)$ and $E_m(2)$, we can calculate the radial force F_r with (28).

$$F_r = \frac{E_m(1) - E_m(2)}{2\Delta r} \tag{28}$$

where $\Delta r = 0.001$ m is the radial distance in length for which the inner cylinder is moved away. The radial stiffness k_r is determined by (29).

$$k_r = \frac{F_r}{\Delta r} \tag{29}$$

The numerical application gives $k_r = 5.6$ N/mm. As a conclusion, for a ferrofluid seal whose thickness equals 0.3 mm, the radial stiffness is $k_r = 5.6$ N/mm.

6.2. Decentering supported by the ferrofluid seal

The determination of the maximum possible decentering depends on the quantity of ferrofluid used in the seal. A numerical application is given here to illustrate that. The ferrofluid quantity we use corresponds to the case when its thickness equals 0.4 mm. With the inner cylinder, the air gap equals 0.3 mm. It is noted that the inner cylinder is radially moved away. As some ferrofluid is moved off from the place where

the ferrofluid seal is crushed, the ferrofluid seal thickness increases at the opposite from the place where the ferrofluid seal is crushed. The moving off centre for which a perforation can appear in the seal corresponds to 0.14 mm. As a conclusion, in this configuration with $r_{in} = 25$ mm, $r_{out} = 28$ mm and $h = 3$ mm, the moving off centre supported by the ferrofluid seal equals 0.14 mm.

7. CONCLUSION

This paper has presented an analytical way of studying analytically the mechanical properties of a ferrofluid seal. This static study is based on the potential energy criterion. Moreover, the magnetic field created by the ring permanent magnets being very intense, the magnetic field created by the magnetic particles is omitted. The expression of the magnetic pressure has been determined analytically and has been plotted in order to see where the potential energy is the most important. The shape of the ferrofluid seal depends on the quantity of ferrofluid which is used and we have shown that for small quantities, the ferrofluid seal contour can be described in terms of an equation of ellipse. Moreover, if the thickness of the ferrofluid seal is greater than 6 mm, the ferrofluid seal spreads over the whole inner faces of the ring permanent magnets. It can be noted that the shape of the ferrofluid seal changes when the inner cylinder is taken into account. This change comes with an energy reduction which depends on the radial displacement of the cylinder, so on the seal crushing. The ferrofluid seal capacity has been determined and we have shown that it depends on the thickness of the ferrofluid seal. At last, a way of obtaining the radial stiffness of a ferrofluid seal is presented and we have found a radial stiffness which equals 5.6 N/mm. Furthermore, the moving off centre supported by the ferrofluid seal has been studied and we have found that it depends on the quantity of ferrofluid used in the seal. These results can be useful to design many engineering and industrial applications which use ferrofluid seals.

REFERENCES

1. R. E. Rosensweig, Y. Hirota, S. Tsuda, and K. Raj, "Study of audio speakers containing ferrofluid," *J. Phys. : Condens. Matter*, vol. 20, 2008.
2. R. E. Rosensweig, *Ferrohydrodynamics*. Dover, 1997.
3. K. Raj, V. Moskowitz, and R. Casciari, "Advances in ferrofluid in ferrofluid technology," *Journal of Magnetism and Magnetic Materials*, vol. 149, pp. 174–180, 1995.

4. S. Babic and C. Akyel, "Improvement in the analytical calculation of the magnetic field produced by permanent magnet rings," *Progress in Electromagnetics Research C*, vol. 5, pp. 71–82, 2008.
5. S. Babic and C. Akyel, "An improvement in the calculation of the magnetic field for an arbitrary geometry coil with rectangular cross section," *International Journal of Numerical Modelling: Electronic Networks, Devices and Fields*, vol. 18, pp. 493–504, November 2005.
6. S. Babic, C. Akyel, and M. M. Gavrilovic, "Calculation improvement of 3d linear magnetostatic field based on fictitious magnetic surface charge," *IEEE Trans. Magn.*, vol. 36, no. 5, pp. 3125–3127, 2000.
7. S. Babic, C. Akyel, S. Salon, and S. Kincic, "New expressions for calculating the magnetic field created by radial current in massive disks," *IEEE Trans. Magn.*, vol. 38, no. 2, pp. 497–500, 2002.
8. S. Babic, C. Akyel, and S. Salon, "New procedures for calculating the mutual inductance of the system: filamentary circular coil-massive circular solenoid," *IEEE Trans. Magn.*, vol. 39, no. 3, pp. 1131–1134, 2003.
9. R. Ravaud, G. Lemarquand, V. Lemarquand, and C. Depollier, "Analytical calculation of the magnetic field created by permanent-magnet rings," *IEEE Trans. Magn.*, vol. 44, no. 8, pp. 1982–1989, 2008.
10. R. Ravaud, G. Lemarquand, V. Lemarquand, and C. Depollier, "Discussion about the analytical calculation of the magnetic field created by permanent magnets.," *Progress in Electromagnetics Research B*, vol. 11, pp. 281–297, 2009.
11. R. Ravaud, G. Lemarquand, V. Lemarquand, and C. Depollier, "The three exact components of the magnetic field created by a radially magnetized tile permanent magnet.," *Progress in Electromagnetics Research, PIER 88*, pp. 307–319, 2008.
12. J. P. Selvaggi, S. Salon, O. M. Kwon, and M. V. K. Chari, "Calculating the external magnetic field from permanent magnets in permanent-magnet motors - an alternative method," *IEEE Trans. Magn.*, vol. 40, no. 5, pp. 3278–3285, 2004.
13. H. S. Choi, Y. S. Kim, K. T. Kim, and I. H. Park, "Simulation of hydrostatical equilibrium of ferrofluid subject to magneto-static field," *IEEE Trans. Magn.*, vol. 44, no. 6, pp. 818–821, 2008.
14. R. C. Shah and M. Bhat, "Ferrofluid squeeze film in a long bearing," *Tribology International*, vol. 37, pp. 441–446, 2004.
15. J. Bajkowski, J. Nachman, M. Shillor, and M. Sofonea, "A model

for a magnetorheological damper," *Mathematical and computer modelling*, vol. 48, pp. 56–68, 2008.

16. G. S. Park and K. Seo, "New design of the magnetic fluid linear pump to reduce the discontinuities of the pumping forces," *IEEE Trans. Magn.*, vol. 40, pp. 916–919, 2004.
17. G. Lemarquand, "Ironless loudspeakers," *IEEE Trans. Magn.*, vol. 43, no. 8, pp. 3371–3374, 2007.
18. R. Ravaud, G. Lemarquand, V. Lemarquand, and C. Depollier, "Ironless loudspeakers with ferrofluid seals," *Archives of Acoustics*, vol. 33, no. 4, pp. 3–10, 2008.
19. M. Berkouk, V. Lemarquand, and G. Lemarquand, "Analytical calculation of ironless loudspeaker motors," *IEEE Trans. Magn.*, vol. 37, no. 2, pp. 1011–1014, 2001.
20. I. Tarapov, "Movement of a magnetizable fluid in lubricating layer of a cylindrical bearing," *Magnetohydrodynamics*, vol. 8, no. 4, pp. 444–448, 1972.
21. J. Walker and J. Backmaster, "Ferrohydrodynamics thrust bearings," *Int. J. Eng. Sci.*, vol. 17, pp. 1171–1182, 1979.
22. N. Tiperi, "Overall characteristics of bearings lubricated ferrofluids," *ASME J. Lubr. Technol.*, vol. 105, pp. 466–475, 1983.
23. Y. L. Raikher, V. I. Stepanov, J. C. Bacri, and R. Perzynski, "Orientational dynamics in magnetic fluids under strong coupling of external and internal relaxations," *Journal of Magnetism and Magnetic Materials*, vol. 289, pp. 222–225, 2005.
24. S. Miyake and S. Takahashi, "Sliding bearing lubricated with ferromagnetic fluid," *ASLE Trans.*, vol. 28, pp. 461–466, 1985.
25. H. Chang, C. Chi, and P. Zhao, "A theoretical and experimental study of ferrofluid lubricated four-pocket journal bearing," *Journal of Magnetism and Magnetic Materials*, vol. 65, pp. 372–374, 1987.
26. Y. Zhang, "Static characteristics of magnetized journal bearing lubricated with ferrofluids," *ASME J. Tribol.*, vol. 113, pp. 533–538, 1991.
27. T. Osman, G. Nada, and Z. Safar, "Static and dynamic characteristics of magnetized journal bearings lubricated with ferrofluid," *Tribology International*, vol. 34, pp. 369–380, 2001.
28. R. C. Shah and M. Bhat, "Anisotropic permeable porous facing abd slip velocity squeeze film in axially undefined journal bearing with ferrofluid lubricant," *Journal of Magnetism and Magnetic Materials*, vol. 279, pp. 224–230, 2004.
29. F. Cunha and H. Couto, "A new boundary integral formulation to

describe three-dimensional motions of interfaces between magnetic fluids," *Applied mathematics and computation*, vol. 199, pp. 70–83, 2008.

30. S. Chen, Q. Zhang, H. Chong, T. Komatsu, and C. Kang, "Some design and prototyping issues on a 20 krpm hdd spindle motor with a ferro-fluid bearing system," *IEEE Trans. Magn.*, vol. 37, no. 2, pp. 805–809, 2001.
31. Q. Zhang, S. Chen, S. Winoto, and E. Ong, "Design of high-speed magnetic fluid bearing spindle motor," *IEEE Trans. Magn.*, vol. 37, no. 4, pp. 2647–2650, 2001.
32. M. Miwa, H. Harita, T. Nishigami, R. Kaneko, and H. Unozawa, "Frequency characteristics of stiffness and damping effect of a ferrofluid bearing," *Tribology Letter*, vol. 15, no. 2, pp. 97–105, 2003.
33. W. Ochonski, "The attraction of ferrofluid bearings," *Mach. Des.*, vol. 77, no. 21, pp. 96–102, 2005.
34. Z. Meng and Z. Jibin, "An analysis on the magnetic fluid seal capacity," *Journal of Magnetism and Magnetic Materials*, vol. 303, pp. e428–e431, 2006.
35. G. Matthies and U. Tobiska, "Numerical simulation of normal-field instability in the static and dynamic case," *Journal of Magnetism and Magnetic Materials*, vol. 289, pp. 436–439, 2005.
36. A. Ivanov, S. Kantorovich, V. Mendelev, and E. Pyanzina, "Ferrofluid aggregation in chains under the influence of a magnetic field," *Journal of Magnetism and Magnetic Materials*, vol. 300, pp. e206–e209, 2006.
37. P. Kuzhir, "Free boundary of lubricant film in ferrofluid journal bearings," *Tribology International*, vol. 41, pp. 256–268, 2008.